

# Ginsenoside Rg1 reduces $\beta$ -amyloid levels by inhibiting CDK5-induced PPAR $\gamma$ phosphorylation in a neuron model of Alzheimer's disease

QIANKUN QUAN<sup>1</sup>, XI LI<sup>1</sup>, JIANJUN FENG<sup>1</sup>, JIXING HOU<sup>2</sup>, MING LI<sup>1</sup> and BINGWEI ZHANG<sup>1</sup>

<sup>1</sup>Department of Geriatrics, The Second Affiliated Hospital of Xi'an Jiaotong University, Xi'an, Shaanxi 710004;

<sup>2</sup>Department of Psychiatry, Xi'an Mental Health Center, Xi'an, Shaanxi 710061, P.R. China

Received February 19, 2020; Accepted July 16, 2020

DOI: 10.3892/mmr.2020.11424

**Abstract.** The accumulation of  $\beta$ -amyloid peptides (A $\beta$ ) in the brain is a hallmark of Alzheimer's disease (AD). Studies have indicated that ginsenoside Rg1, a primary component of ginseng (*Panax ginseng*), reduces brain A $\beta$  levels in an AD model through peroxisome proliferator-activated receptor  $\gamma$  (PPAR $\gamma$ ), thereby regulating the expression of insulin-degrading enzyme (*Ide*) and  $\beta$ -amyloid cleavage enzyme 1 (*Bace1*), which are PPAR $\gamma$  target genes. However, the effects of ginsenoside Rg1 on PPAR $\gamma$  remain unclear. Since cyclin-dependent kinase 5 (CDK5) mediates PPAR $\gamma$  phosphorylation in adipose tissue, this study aimed to investigate whether ginsenoside Rg1 regulates PPAR $\gamma$  target genes and reduces A $\beta$  levels by inhibiting PPAR $\gamma$  phosphorylation through the CDK5 pathway. In the present study, a model of AD was established by treating primary cultured rat hippocampal neurons with A $\beta$ <sub>1-42</sub>. The cells were pretreatment with ginsenoside Rg1 and roscovitine, a CDK5-inhibitor, prior to the treatment with A $\beta$ <sub>1-42</sub>. Neuronal apoptosis was detected using TUNEL staining. PPAR $\gamma$  phosphorylation and protein expression levels of PPAR $\gamma$ , CDK5, IDE, BACE1, amyloid precursor protein (APP) and A $\beta$ <sub>1-42</sub> were measured by western blotting. The mRNA expression levels of PPAR $\gamma$ , CDK5, IDE, BACE1 and APP were assessed using reverse transcription-quantitative PCR. The results of the present study demonstrated that in an AD model induced by A $\beta$ <sub>1-42</sub>, ginsenoside Rg1 significantly decreased CDK5 expression, inhibited PPAR $\gamma$  phosphorylation at serine 273, elevated IDE expression, downregulated BACE1 and APP expression, decreased A $\beta$ <sub>1-42</sub> levels and attenuated neuronal apoptosis. The CDK5 inhibitor, roscovitine, demonstrated similar effects.

These results suggest that ginsenoside Rg1 has neuroprotective properties and has potential for use in the treatment of AD.

## Introduction

Ginseng (*Panax ginseng*), which is documented in Shennong's Classic of Materia Medica as having intellect-enhancing effects, has been widely used in China for millennia (1). Ginsenoside Rg1, a primary ginseng components, has multiple neuroprotective effects against Alzheimer's disease (AD), including the improvement of memory impairment (2), inhibition of neuronal apoptosis (3), amelioration of oxidative stress (4) and attenuation of mitochondrial dysfunction (5). The accumulation of  $\beta$ -amyloid peptides (A $\beta$ ) is the most prominent pathological feature of AD and significantly influences the pathogenesis of the disease (6). The aggregation and accumulation of A $\beta$  in the brain may lead to neuroinflammatory responses (7), neurofibrillary tangle formation (8), synaptic loss (9), oxidative stress (10), neuronal apoptosis (11), cholinergic dysfunction (12) and tau phosphorylation (13). It has been reported that ginsenoside Rg1 has A $\beta$ -scavenging effects, for example, ginsenoside Rg1 inhibits the transcription and translation of  $\beta$ -amyloid cleavage enzyme 1 (*Bace1*), a target gene of peroxisome proliferator-activated receptor  $\gamma$  (PPAR $\gamma$ ), by enhancing the binding of PPAR $\gamma$  to the *Bace1* promoter, thereby decreasing BACE1 activity, which ultimately attenuates A $\beta$  production (14). Additionally, ginsenoside Rg1 upregulates PPAR $\gamma$  expression in the rat hippocampus AD model, thereby increasing the expression of insulin-degrading enzyme (*Ide*) (another PPAR $\gamma$  target gene) and promoting the clearance of A $\beta$ <sub>1-42</sub> from the hippocampus (15). These studies suggest that PPAR $\gamma$  is involved in the reduction of A $\beta$  levels caused by ginsenoside Rg1; however, the mechanisms by which ginsenoside Rg1 affects PPAR $\gamma$  remain unclear.

Cyclin-dependent kinase 5 (CDK5), a cyclin-dependent kinase, is a proline-directed serine/threonine kinase predominantly activated in post-mitotic cells and has various activities including cytoskeletal dynamics, signaling cascades, gene expression, cell survival, neurodevelopment and brain function (16-19). Phosphorylation is an important post-translational modification of PPAR $\gamma$ . It has been demonstrated that in the adipose tissue, CDK5 induces PPAR $\gamma$  phosphorylation

**Correspondence to:** Professor Xi Li, Department of Geriatrics, The Second Affiliated Hospital of Xi'an Jiaotong University, 157 Xiwu Road, Xi'an, Shaanxi 710004, P.R. China  
E-mail: lixi2100@163.com

**Key words:** ginsenoside Rg1, Alzheimer's disease, amyloid precursor protein, peroxisome proliferator-activated receptors, cyclin-dependent kinase 5

at serine 273 (Ser273), which is located in the hinge region between the DNA- and the ligand-binding domains *in vivo* and *in vitro* (20). Furthermore, our previous study demonstrated that in rat primary hippocampal neurons CDK5 regulates the expression of IDE and BACE1 by mediating the phosphorylation of PPAR $\gamma$ , resulting in decreased A $\beta$  clearance and increased A $\beta$  production (21). The present study aimed to investigate whether ginsenoside Rg1 inhibits the phosphorylation of PPAR $\gamma$  through the downregulation of the CDK5 pathway. The findings of this study will deepen the understanding of the neuroprotective properties of ginsenoside Rg1 and its potential use in the treatment of AD.

## Materials and methods

**Reagents.** Ginsenoside Rg1 (molecular formula: C<sub>42</sub>H<sub>72</sub>O<sub>14</sub>; molecular weight: 801.01; HPLC purity: 98%) was purchased from Baoji Herbest Bio-Tech Co., Ltd. A $\beta$ <sub>1-42</sub> and roscovitine were purchased from Sigma Aldrich; Merck KGaA. Rabbit anti-rat IDE (cat. no. ab133561), BACE1 (cat. no. ab10716) and amyloid precursor protein (APP; cat. no. ab15272) polyclonal antibodies were purchased from Abcam. Rabbit anti-rat p-PPAR $\gamma$ -Ser273 polyclonal antibody (cat. no. bs-4888R) was purchased from BIOSS Antibodies. Rabbit anti-rat CDK5 (cat. no. WL01673), PPAR $\gamma$  (cat. no. WL0269) and A $\beta$ <sub>1-42</sub> (cat. no. WL01427) polyclonal antibodies, anti- $\beta$ -actin antibody (cat. no. WL01845), goat anti-rabbit secondary horse-radish peroxidase-conjugated antibody (cat. no. WLA023), TUNEL assay kit, total protein extraction kit, bicinchoninic acid (BCA) protein assay kit and enhanced chemiluminescence (ECL) reagent were purchased from Wanleibio Co., Ltd. Dulbecco's modified Eagle's medium (DMEM) was purchased from Gibco; Thermo Fisher Scientific, Inc. Fetal bovine serum (FBS) was purchased from Biological Industries. Trypsin and 4',6-diamidino-2-phenylindole (DAPI) were purchased from Beyotime Institute of Biotechnology. TRIzol<sup>®</sup> and 2X Power Taq PCR MasterMix were purchased from BioTeke Corporation. SYBR Green master mix was purchased from Beijing Solarbio Science & Technology Co., Ltd.

**Isolation and culture of rat hippocampal neurons.** Rat hippocampal neurons were isolated and cultured using the methods previously described (22). In total, 150 2-day-old Sprague Dawley rats (weight, 8 $\pm$ 2 g; males, 75; females, 75) were used in the study. These rats were obtained from the Experimental Animal Center of Xi'an Jiaotong University Health Science Center [License no. SCXK (Shaan) 2018-001], which were housed in a specific-pathogen free facility maintained at 23°C with a 12-h light-dark cycle and 24-h atmosphere purification, and were allowed free access to breastmilk from their mother. In brief, brain tissues were isolated from these rats under aseptic conditions. The hippocampal tissues were then dissected on an ultra-clean bench, cut into pieces, and digested by trypsin. Subsequently, DMEM containing 10% FBS and penicillin/streptomycin was added for trypsin neutralization. Cell suspension was repeatedly digested five-six times after centrifugation (168 x g, 7 min, 25°C). After filtration and centrifugation, the hippocampal neurons were placed in a poly-lysine-coated 6-well plate at a density of 5x10<sup>5</sup> cells/ml and cultured for 8 h at 37°C with 5% CO<sub>2</sub>

and saturated humidity. Subsequently, the culture medium was changed to neurobasal medium containing 2% B27, 0.5 mM glutamine, 100 U/ml penicillin, and 100 U/ml streptomycin and the cells were cultured for 48 h. Cytarabine was then added to the medium (final concentration, 10  $\mu$ M) to inhibit the growth of glial cells. The media were changed once every 3 days until maturation and network formation of the hippocampal neurons in ~15 days. All experimental procedures in this study were approved by the Ethics Committee of The Second Affiliated Hospital of Xi'an Jiaotong University (Shaanxi, China).

**Drug treatment.** The cultured neurons were divided into the following three groups: Control, model and ginsenoside Rg1 (Rg1) groups. The control group was used as the vehicle treated group, in which no drugs were added to the culture medium; in the model group, cultured neurons were treated with 8  $\mu$ M A $\beta$ <sub>1-42</sub> (23) for 24 h at 37°C; in the Rg1 group, the cultured neurons were exposed to 60  $\mu$ M ginsenoside Rg1 (24) for 1 h at 37°C and then to 8  $\mu$ M A $\beta$ <sub>1-42</sub> for 24 h at 37°C. To confirm whether ginsenoside Rg1 regulates PPAR $\gamma$  phosphorylation by acting on CDK5, the effects of ginsenoside Rg1 on cultured neurons that were treated with A $\beta$ <sub>1-42</sub> after CDK5 expression was inhibited using the CDK5 inhibitor roscovitine were investigated. Neurons were divided into the three following groups: Model, roscovitine and roscovitine+Rg1 groups. In the model group, the cultured neurons were treated with 8  $\mu$ M A $\beta$ <sub>1-42</sub> for 24 h at 37°C; in the roscovitine group, the cultured neurons were first exposed to 25  $\mu$ M roscovitine (25) for 1 h at 37°C and then to 8  $\mu$ M A $\beta$ <sub>1-42</sub> for 24 h at 37°C; in the roscovitine+Rg1 group, cultured neurons were first treated with 25  $\mu$ M roscovitine for 0.5 h at 37°C followed by 60  $\mu$ M ginsenoside Rg1 for 1 h at 37°C and subsequently 8  $\mu$ M A $\beta$ <sub>1-42</sub> for 24 h at 37°C.

**TUNEL staining.** TUNEL staining was performed using an assay kit according to the manufacturer's instructions. After the slides were fixed with 4% paraformaldehyde at 25°C for 10 min, the cells were permeabilized with 50  $\mu$ l of 0.1% Triton X-100 for 15 min at 25°C. After being washed with phosphate-buffered saline (PBS), the cells were incubated with the TUNEL reaction mixture (formulated by mixing the enzyme and label solutions at a ratio of 1:9) in a wet chamber in the dark at 37°C for 60 min. Subsequently, the cells were washed with PBS and counterstained with DAPI in the dark at 25°C for 5 min. After washing with PBS again, the slides were mounted using mounting medium with anti-fluorescent quenchers. The neurons were counted in a blind manner by two pathologists under a BX 53 fluorescence microscope (Olympus Corporation) at x400 magnification.

The average number of neurons from four random fields of view was used as the final result for each pathologist. The results from the two pathologists were averaged and used to calculate the percentage of TUNEL-positive neurons.

**Western blotting.** Total proteins of the neurons were extracted using the total protein extraction kit according to the manufacturer's instructions and the protein concentration was measured using the BCA protein assay method. After denaturation at 95°C for 5 min, 20  $\mu$ l protein sample (including 40  $\mu$ g protein) was added into each electrophoretic lane,

Table I. Primers used for reverse transcription-quantitative PCR.

Gene	Primer sequence (5'→3')	Primer length	Temperature, °C	PCR product length, bp
Cyclin-dependent kinase 5	F: GGACACCGACTGAGGAAC	18	52.0	103
	R: TTGGGCACGACATTCAC	17	52.5	
Peroxisome proliferator-activated receptor $\gamma$	F: TACCACGGTTGATTTCTC	18	47.7	155
	R: AATAATAAGGCGGGGACG	18	55.3	
Insulin-degrading enzyme	F: TCCCGTGAAGCGACTGT	17	54.3	180
	R: GACTTGTCCGTGGTGGG	17	53.6	
$\beta$ -amyloid cleavage enzyme 1	F: TCCGCATCACCATCCTT	17	54.0	123
	R: TGACCGCTCCCATAACG	17	55.1	
Amyloid precursor protein	F: ACTCTGTGCCAGCCAATA	18	51.2	158
	R: TGAATCATGTCCGAACCTCC	19	53.0	
$\beta$ -actin	F: GGAGATTACTGCCCTGGCTCCTAGC	25	60.1	155
	R: GGCCGGACTCATCGTACTCCTGCTT	25	62.0	

F, Forward; R, Reverse; bp, base pairs.

separated in an 8% sodium dodecyl sulfate-polyacrylamide gel electrophoresis and transferred to a nitrocellulose (NC) membrane. The membrane was blocked with 5% non-fat powdered milk at 37°C for 1 h and was then incubated with rabbit anti-rat CDK5 (1:500), p-PPAR $\gamma$ -Ser273 (1:500), PPAR $\gamma$  (1:400), IDE (1:900), BACE1 (1:600), APP (1:800), and A $\beta$ <sub>1-42</sub> (1:500) polyclonal antibodies overnight at 4°C. After being washed with Tris-buffered saline buffer with 0.05% Tween 20, the NC membrane was incubated with the secondary horseradish peroxidase-conjugated antibody (goat anti-rabbit, 1:1,000) at 37°C for 45 min. Subsequently, the NC membrane was developed using ECL reagent and the blots were scanned. The optical densities of the target bands were analyzed using Gel-Pro Analyzer software (version 4.0, Media Cybernetics, Inc.).

**Reverse transcription-quantitative (RT-q)PCR.** Total RNA from the neurons of the three groups was extracted using TRIzol and the concentrations were measured using a UV spectrophotometer. Reverse transcription was performed according to the manufacturer's instructions. In brief, each RNA sample was added into a nuclease-free centrifuge tube in an ice bath based on the concentration of the extracted RNA sample (consistent RNA concentrations during sample loading), followed by the addition of 1  $\mu$ l of oligo (dT)<sub>15</sub>, 1  $\mu$ l of random primers, and a sufficient volume of double-distilled water to reach a total volume of 12.5  $\mu$ l. The mixture was incubated at 70°C for 5 min and was then rapidly cooled on ice for 2 min. After centrifugation (671 x g, 1 min, 4°C), the reaction mixture was mixed with 2  $\mu$ l of deoxynucleoside triphosphate (2.5 mM each), 4  $\mu$ l of 5X buffer, 0.5  $\mu$ l of RNase inhibitor and 1  $\mu$ l of Moloney-murine leukemia virus (200 U), and was then sequentially subjected to the following conditions: 25°C for 10 min, 42°C for 50 min and 80°C for 10 min to terminate the reaction. The resultant cDNA was stored at -20°C for further use. Primers (Table I) of rat *Cdk5*, *Ppar $\gamma$* , *Ide*, *Bace1* and *App* genes were designed using Primer Premier 5.0

(Premier Biosoft International). All primers were synthesized by Sangon Biotech Co., Ltd. Fluorescence-based RT-qPCR was performed using a 2X Power Taq PCR Master Mix kit with a Exicycler™ 96 real-time PCR instrument (Bioneer Corp.). The PCR reaction was performed according to the manufacturer's instructions in a 20  $\mu$ l mixture including 1  $\mu$ l of cDNA, 0.5  $\mu$ l of the forward primer (10  $\mu$ M), 0.5  $\mu$ l of the reverse primer (10  $\mu$ M), 10  $\mu$ l of the SYBR Green Master Mix and sufficient double-distilled water. Reaction conditions were as follows: Initial denaturation at 94°C for 5 min, followed by denaturation at 94°C for 10 sec, annealing at 60°C for 20 sec and extension at 72°C for 30 sec for 40 cycles. Relative mRNA expression levels were calculated using the 2<sup>- $\Delta\Delta$ C<sub>q</sub></sup> method (26).  $\beta$ -actin was used as the internal control.

**Data analysis.** All data are expressed as the mean  $\pm$  SEM. One-way analysis of variance (ANOVA) followed by a Least Significant Difference post hoc test was performed for multiple comparisons. Statistical analyses were conducted using SPSS (version 16.0, SPSS, Inc.). P<0.05 was considered to indicate a statistically significant difference.

## Results

**Ginsenoside Rg1 inhibits PPAR $\gamma$  phosphorylation in the AD model.** In primary cultured rat hippocampal neurons A $\beta$ <sub>1-42</sub> treatment significantly enhanced PPAR $\gamma$  phosphorylation at Ser273, increased the p-PPAR $\gamma$ /PPAR $\gamma$  ratio and decreased PPAR $\gamma$  protein and mRNA expression levels compared with those in the control group (P<0.05; Fig. 1). These results suggested the presence of PPAR $\gamma$  phosphorylation in the AD neuron model induced by A $\beta$ <sub>1-42</sub>. In addition, pretreatment with ginsenoside Rg1 significantly attenuated the aforementioned A $\beta$ <sub>1-42</sub>-induced effects in these neurons (P<0.05; Fig. 1). Notably, after inhibiting CDK5 expression using roscovitine, the results demonstrated that compared with those in the model group PPAR $\gamma$  phosphorylation was

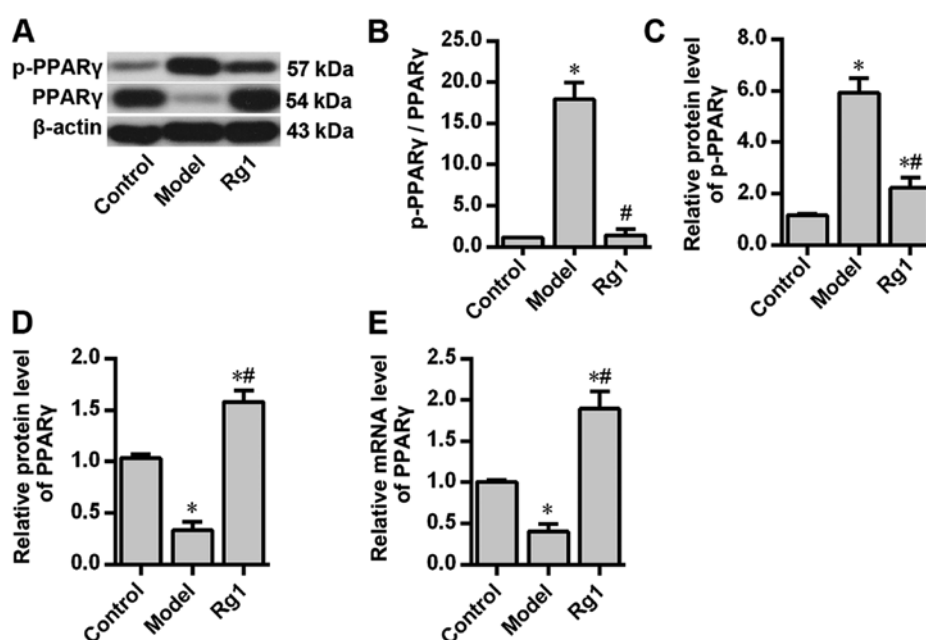


Figure 1. Effects of ginsenoside Rg1 on PPAR $\gamma$  phosphorylation in the Alzheimer's disease neuron model. (A) Western blots for p-PPAR $\gamma$ -Ser273 and PPAR $\gamma$ . (B) Comparison of the p-PPAR $\gamma$ -Ser273/PPAR $\gamma$  ratios among the three groups. (C) Comparison of the p-PPAR $\gamma$ -Ser273 levels among the three groups. Comparison of the PPAR $\gamma$  (D) protein and (E) mRNA expression levels among the three groups. n=6. \*P<0.05 vs. control group; #P<0.05 vs. model group. PPAR $\gamma$ , peroxisome proliferator-activated receptor  $\gamma$ ; Ser, serine.

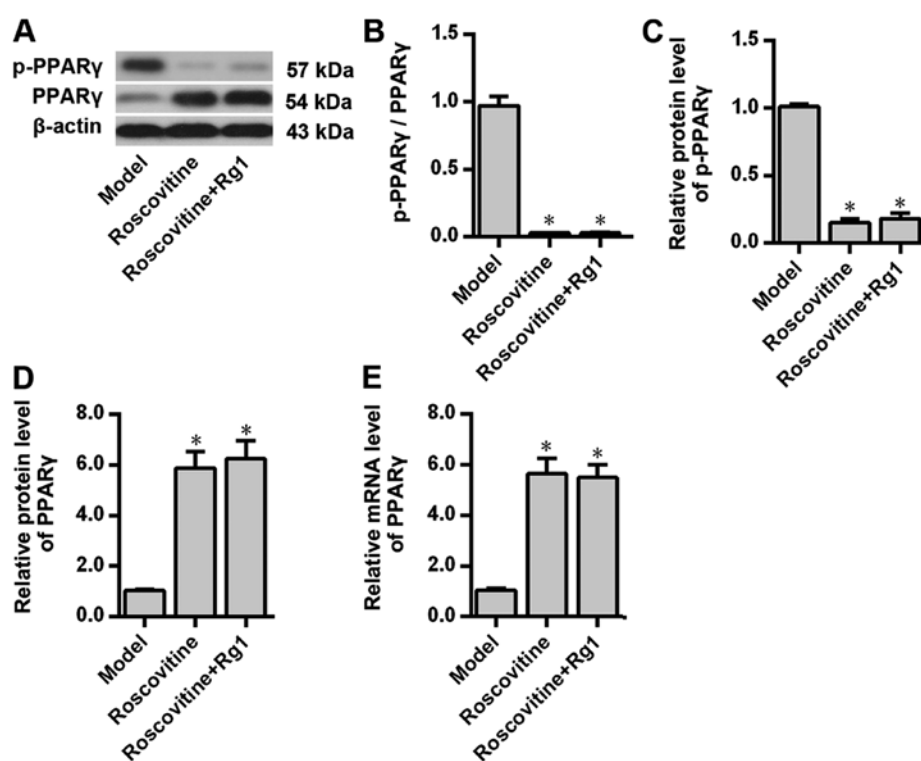


Figure 2. Effects of ginsenoside Rg1 on PPAR $\gamma$  phosphorylation in the Alzheimer's disease neuron model after cyclin-dependent kinase 5 inhibition. (A) Western blots for p-PPAR $\gamma$ -Ser273 and PPAR $\gamma$ . (B) Comparison of the p-PPAR $\gamma$ -Ser273/PPAR $\gamma$  ratios among the three groups. (C) Comparison of the p-PPAR $\gamma$ -Ser273 protein expression levels among the three groups. Comparison of the PPAR $\gamma$  (D) protein and (E) mRNA expression levels among the three groups. n=6. \*P<0.05 vs. model group. PPAR $\gamma$ , peroxisome proliferator-activated receptor  $\gamma$ ; Ser, serine.

significantly inhibited and PPAR $\gamma$  expression levels were significantly increased in the A $\beta_{1-42}$ -treated neurons (P<0.05; Fig. 2). Additionally, PPAR $\gamma$  phosphorylation and the expression levels of PPAR $\gamma$  protein in the A $\beta_{1-42}$ -treated neurons

were not further affected by ginsenoside Rg1 treatment after CDK5 inhibition (P>0.05; Fig. 2), suggesting that CDK5 may be involved in the inhibition of PPAR $\gamma$  phosphorylation induced by ginsenoside Rg1.

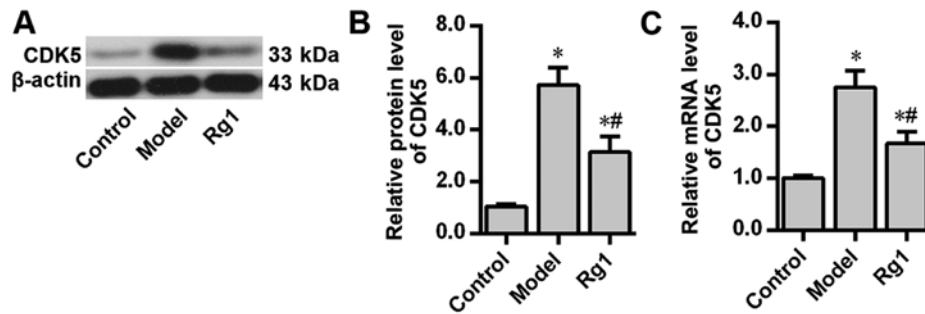


Figure 3. Effects of ginsenoside Rg1 on CDK5 expression levels in the Alzheimer's disease neuron model. (A) Western blots for CDK5. Comparison of the CDK5 (B) protein and (C) mRNA expression levels among the three groups. n=6. \*P<0.05 vs. control group; ##P<0.05 vs. model group. CDK5, cyclin-dependent kinase 5.

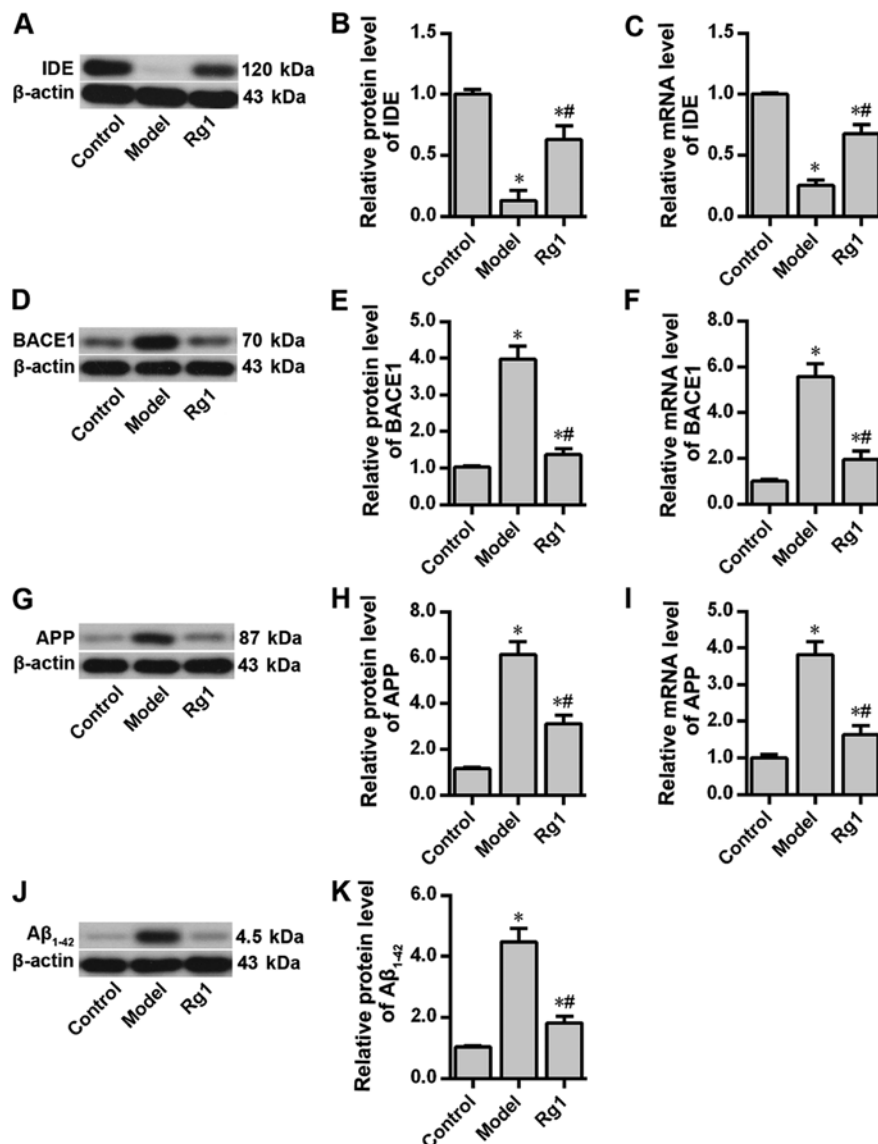


Figure 4. Effects of ginsenoside Rg1 on the expression levels of PPARγ target genes and intracellular Aβ<sub>1-42</sub> levels in the Alzheimer's disease neuron model. Protein expression levels of (A) IDE, (D) BACE1, (G) APP and (J) Aβ<sub>1-42</sub> were assessed by western blotting analysis. IDE (B) protein and (C) mRNA expression levels, BACE1 (E) protein and (F) mRNA expression levels, APP (H) protein and (I) mRNA expression levels, and (K) Aβ<sub>1-42</sub> protein expression levels were compared among the three groups. n=6. \*P<0.05 vs. control group; ##P<0.05 vs. model group. PPARγ, peroxisome proliferator-activated receptor γ; IDE, insulin-degrading enzyme; BACE1, β-amyloid cleavage enzyme 1; APP, amyloid precursor protein; Aβ, β-amyloid peptides.

*Ginsenoside Rg1 decreases CDK5 expression levels in the AD model.* The effects of ginsenoside Rg1 on CDK5 expression

in the neuron model of AD were investigated. Western blotting and RT-qPCR analyses demonstrated that in the primary

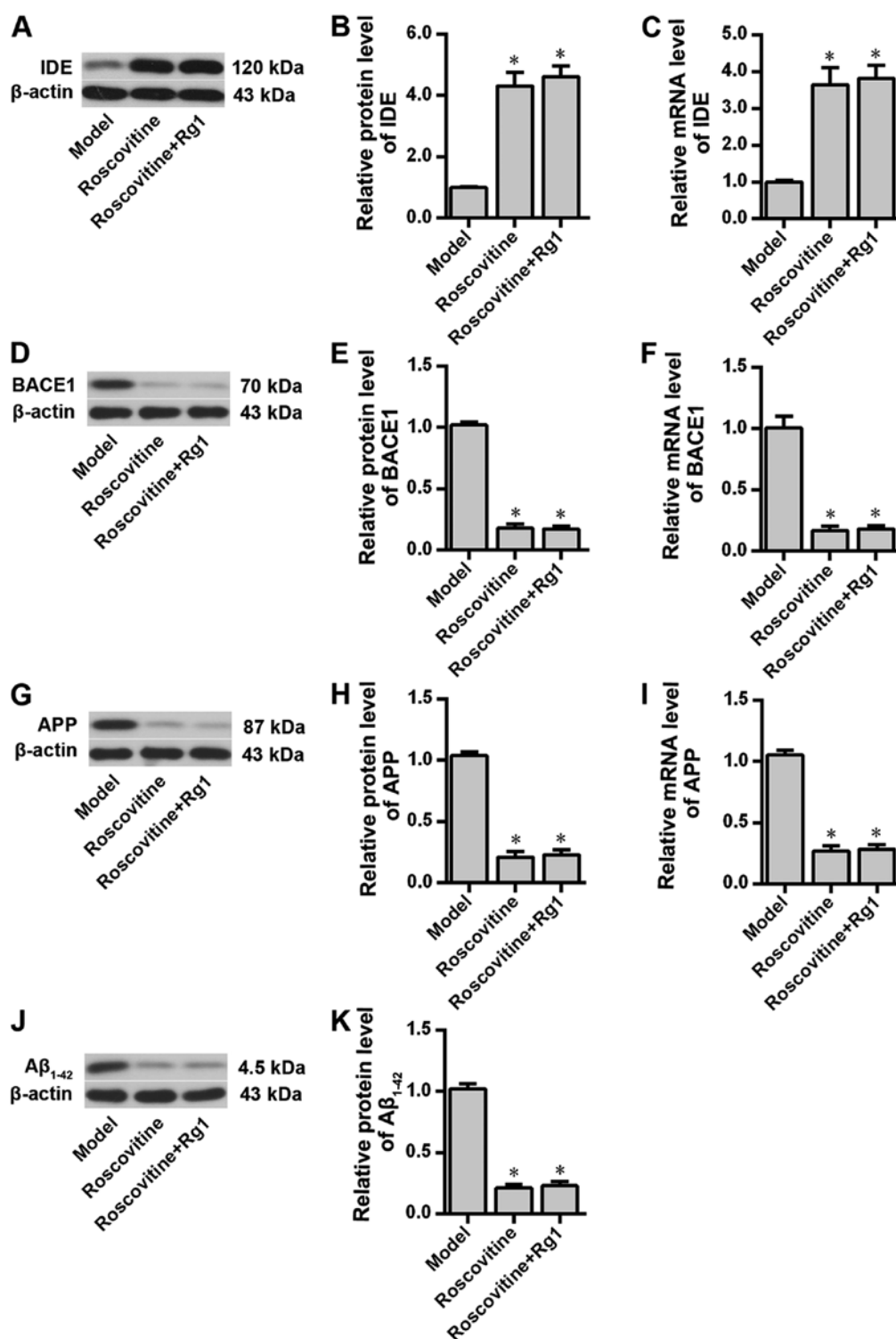


Figure 5. Effects of ginsenoside Rg1 on the expression levels of PPAR $\gamma$  target genes and intracellular A $\beta_{1-42}$  levels in the Alzheimer's disease neuron model after CDK5 inhibition. Protein expression levels of (A) IDE, (D) BACE1, (G) APP and (J) A $\beta_{1-42}$  were assessed by western blotting analysis. IDE (B) protein and (C) mRNA expression levels, BACE1 (E) protein and (F) mRNA expression levels, APP (H) protein and (I) mRNA expression levels and (K) A $\beta_{1-42}$  protein expression levels were compared among the three groups. n=6. \*P<0.05 vs. model group. PPAR $\gamma$ , peroxisome proliferator-activated receptor  $\gamma$ ; IDE, insulin-degrading enzyme; BACE1,  $\beta$ -amyloid cleavage enzyme 1; APP, amyloid precursor protein; A $\beta$ ,  $\beta$ -amyloid peptides.

cultured rat hippocampal neurons A $\beta_{1-42}$  treatment significantly increased the protein and mRNA expression levels of CDK5 compared with those in the control group (P<0.05); but, ginsenoside Rg1 pretreatment significantly attenuated the A $\beta_{1-42}$ -induced increase in the protein and mRNA expression levels of CDK5 (P<0.05; Fig. 3).

*Ginsenoside Rg1 regulates the expression of PPAR $\gamma$  target genes and decreases intracellular A $\beta_{1-42}$  levels in the AD model.* The effects of ginsenoside Rg1 on the expression of PPAR $\gamma$  target genes and intracellular A $\beta_{1-42}$  level when CDK5 was inhibited were examined. The results demonstrated that compared with the rat hippocampal neurons in the control



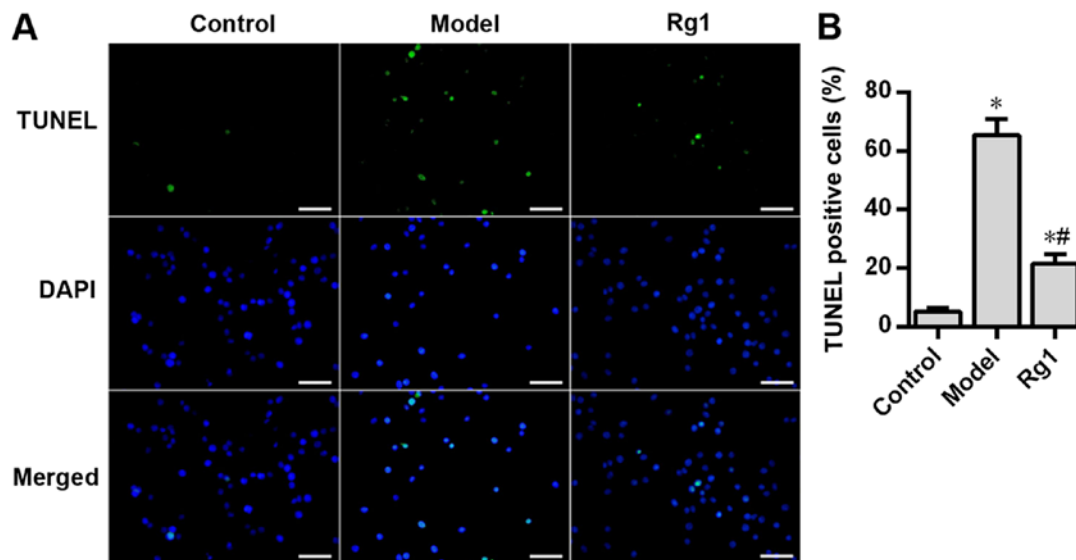


Figure 6. Effects of ginsenoside Rg1 on  $\beta$ -amyloid peptides1-42-induced apoptosis in rat hippocampal neurons. (A) TUNEL staining. Green spots represent TUNEL-positive nuclei and blue spots represent DAPI-counterstained nuclei. Scale bar, 50  $\mu$ m. (B) Comparison of the percentages of TUNEL-positive neurons among the three groups. n=6. \*P<0.05 vs. control group; #P<0.05 vs. model group. TUNEL, transferase dUTP nick end-labeling.

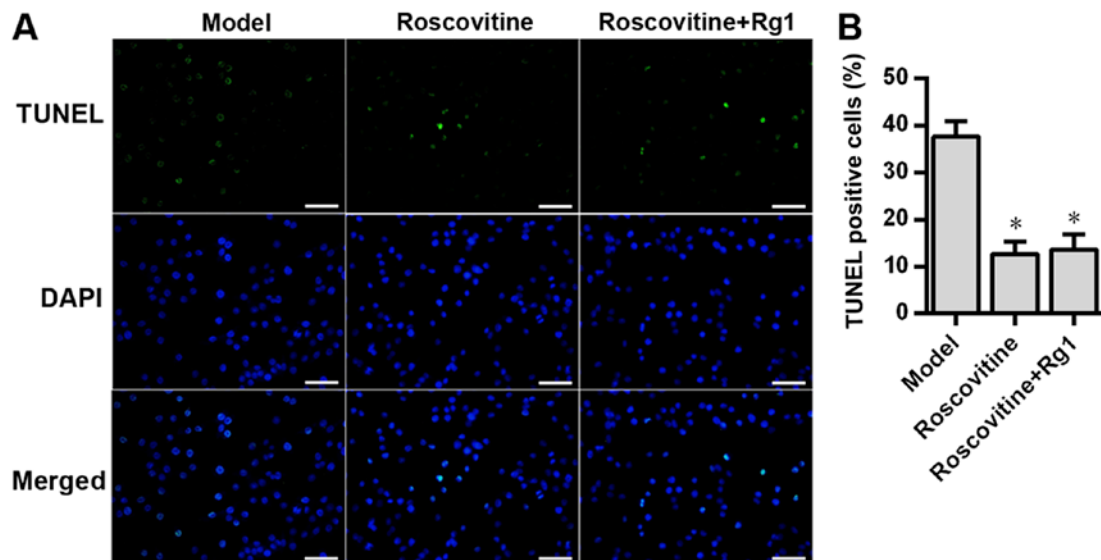


Figure 7. Effects of ginsenoside Rg1 on  $\beta$ -amyloid peptides1-42-induced apoptosis in rat hippocampal neurons after cyclin-dependent kinase 5 inhibition. (A) TUNEL staining. Green spots represent TUNEL-positive nuclei and blue spots represent DAPI-counterstained nuclei. Scale bar, 50  $\mu$ m. (B) Comparison of the percentages of TUNEL-positive neurons among the three groups. n=6. \*P<0.05 vs. model group. TUNEL, transferase dUTP nick end-labeling.

group, those in the model group exhibited significantly decreased IDE protein and mRNA expression levels (P<0.05), but significantly increased BACE1, APP and enhanced intracellular  $A\beta_{1-42}$  levels (P<0.05; Fig. 4). Additionally, pretreatment with ginsenoside Rg1 significantly attenuated  $A\beta_{1-42}$ -induced effects in these neurons (P<0.05; Fig. 4). Additionally, compared with those in the model group inhibition of CDK5 expression using roscovitine significantly increased the expression levels of IDE and reduced the expression levels of BACE1, APP and  $A\beta_{1-42}$  in rat hippocampal neurons treated with  $A\beta_{1-42}$  (P<0.05; Fig. 5). In addition, no significant differences were observed in the expression levels of IDE, BACE1, APP and  $A\beta_{1-42}$  after ginsenoside Rg1 treatment following CDK5 inhibition with roscovitine (P>0.05; Fig. 5).

*Ginsenoside Rg1 attenuates  $A\beta_{1-42}$ -induced apoptosis in rat hippocampal neurons.* In the present study, TUNEL staining was performed to determine the effects of  $A\beta_{1-42}$  and ginsenoside Rg1 on the apoptosis of rat hippocampal neurons. Compared with that in the control group,  $A\beta_{1-42}$  treatment significantly increased neuronal apoptosis in the model group (P<0.05; Fig. 6), but pretreatment with ginsenoside Rg1 significantly decreased  $A\beta_{1-42}$ -induced neuronal apoptosis (P<0.05; Fig. 6). In addition, the neuronal apoptosis rate in the roscovitine group was significantly lower compared with that in the model group (P<0.05; Fig. 7). Additionally, no significant difference was observed in the neuronal apoptosis rate between the roscovitine group and the roscovitine+Rg1 group (P>0.05; Fig. 7).

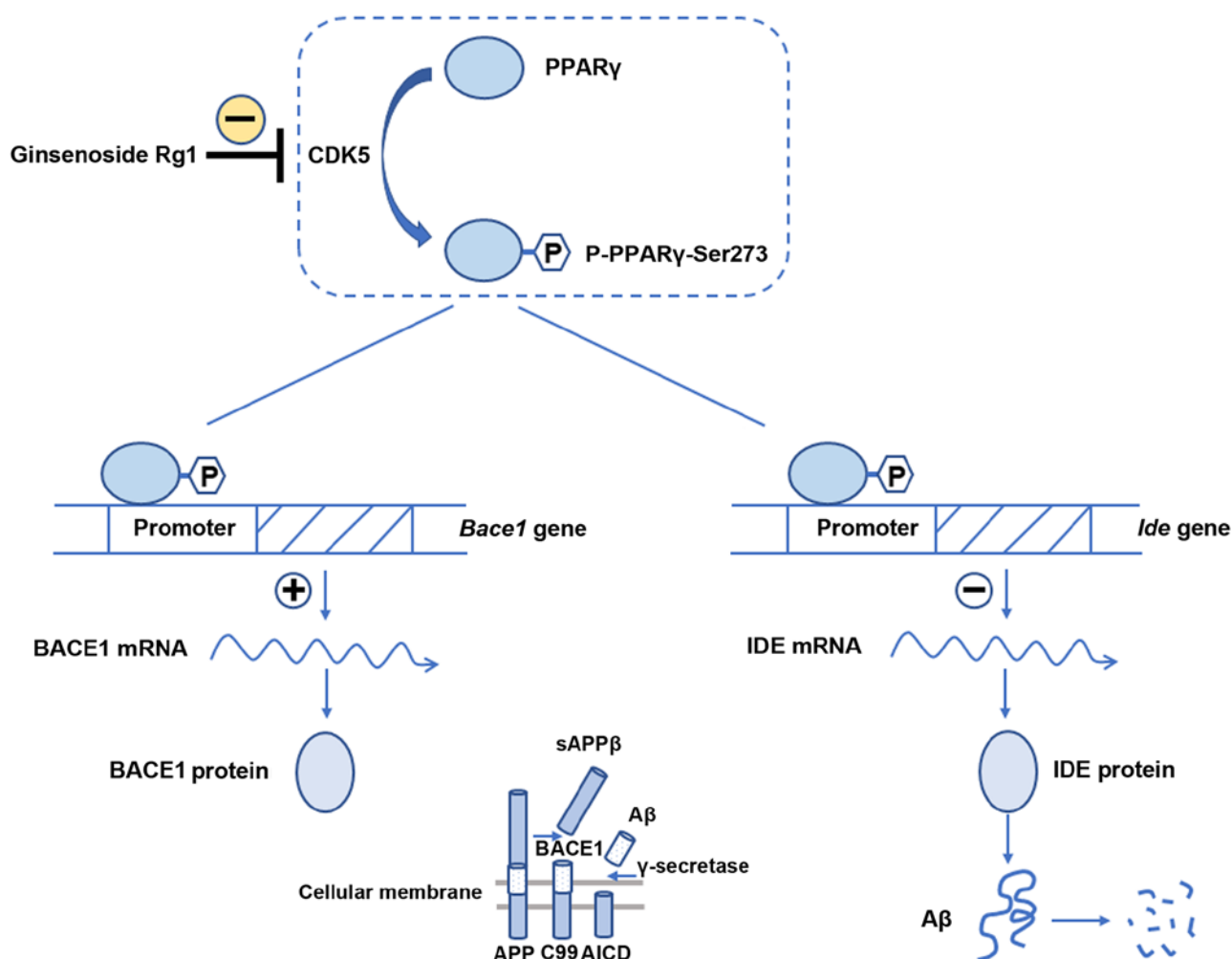


Figure 8. The possible mechanisms by which ginsenoside Rg1 reduces A $\beta$  level by affecting PPAR $\gamma$ . *Ide* and *Bace1* are PPAR $\gamma$  target genes. IDE degrades A $\beta$  directly, whereas BACE1 proteolyzes APP to produce soluble  $\beta$ -fragment of the amyloid precursor protein and C-terminal fragment containing 99 amino acids, which is then enzymatically cleaved by  $\gamma$ -secretase to generate A $\beta$ . CDK5 downregulate the expression of IDE and upregulate the expression of BACE1 by mediating PPAR $\gamma$  phosphorylation at Ser273. The results of the present study demonstrated that ginsenoside Rg1 inhibited PPAR $\gamma$  phosphorylation at Ser273 by downregulating the expression of CDK5, thereby affecting the expression of IDE and BACE1 and decreasing A $\beta$  levels. A $\beta$ ,  $\beta$ -amyloid peptides; PPAR $\gamma$ , peroxisome proliferator-activated receptor  $\gamma$ ; IDE, insulin-degrading enzyme; BACE1,  $\beta$ -amyloid cleavage enzyme 1; CDK5, cyclin-dependent kinase 5; Ser, serine.

## Discussion

This study investigated whether ginsenoside Rg1 inhibits the phosphorylation of PPAR $\gamma$  through the downregulation of the CDK5 pathway, thereby affecting the expression of PPAR $\gamma$  target genes *Bace1* and *Ide* and reducing A $\beta$  levels (Fig. 8). PPARs are ligand-activated nuclear transcription factors, which regulate the transcription of target genes by binding to the peroxisome proliferator response element (PPRE) located on the promoters of these genes (27). Different types of fatty acids (FAs), including docosahexaenoic acid, activate PPARs in adipose tissues (28,29). FA binding to PPARs control the transcription of specific genes including those encoding for various metabolic and cellular processes such as FA  $\beta$ -oxidation and adipogenesis, making them key mediators of lipid homeostasis (29). PPAR $\gamma$  is one of PPARs superfamily members (along with PPAR $\alpha$ , PPAR $\beta/\delta$ ). A previous study has reported that PPAR $\gamma$  inhibits BACE1 expression by binding to the PPRE on the *Bace1* gene promoter in N2a/APP695 cells (30), which is an essential enzyme in the generation

of A $\beta$  as it hydrolyzes APP to form A $\beta$  (31). Additionally, PPAR $\gamma$  also bind to the PPRE in the *Ide* promoter, thereby regulating *Ide* gene transcription and promoting IDE protein expression (32), which has been demonstrated to degrade A $\beta$  (33). These findings indicate that PPAR $\gamma$  serves a key role in the inhibition of A $\beta$  generation and the promotion of A $\beta$  degradation. Moreover, PPAR $\gamma$  has anti-inflammatory effects through inhibiting the generation of certain proinflammatory cytokines (such as tumor necrosis factor, interleukin-1 $\beta$  and interleukin-6), the production of nitric oxide, and the expression of matrix metalloproteinase 9 and macrophage scavenger receptor 1 (34). Studies have reported that these molecules are closely associated with the onset of AD (35-40). Furthermore, oxidative stress usually occurs during early stages of AD and elevates with increased AD severity (41); PPAR $\gamma$  inhibits A $\beta$ -induced oxidative stress (42). Therefore, PPAR $\gamma$  agonists may provide neuroprotective effects against AD.

Several clinical and experimental studies have investigated the role of thiazolidinediones (TZDs), PPAR $\gamma$  agonists, in AD, for example, pioglitazone reduces brain A $\beta$  levels (43)



and improves learning and memory in APP/PS1 mice (44), and decreases tau phosphorylation (45) and neuronal apoptosis (46) in an AD cell model; rosiglitazone decreases A $\beta$ <sub>1-40</sub> and A $\beta$ <sub>1-42</sub> levels, reduces tau phosphorylation, alleviates memory impairment (47), and inhibits A $\beta$ -induced oxidative stress (48), inflammatory responses (49) and mitochondrial dysfunction (50) in both *in vitro* and *in vivo* systems. Oral administration of rosiglitazone improves cognitive function in patients with mild-to-moderate AD (51). Troglitazone and ciglitazone prevent A $\beta$ -induced microglial- and monocyte-mediated neurotoxicity and inhibit A $\beta$ -induced increased expression of interleukin 6, tumor necrosis factor  $\alpha$ , and cyclooxygenase-2 (52). Recently, a study demonstrated that pioglitazone inhibits the phosphorylation of PPAR $\gamma$  at Ser273 *in vitro* by inhibiting CDK5 expression, which in turn affected the expression of PPAR $\gamma$  target genes *Ide* and *Bace1*, thereby promoting A $\beta$  degradation and reducing A $\beta$  production. This reduced A $\beta$  levels in the brain, thereby exerting neuroprotective effects in an AD model (53). These findings indicate that TZDs have neuroprotective effects against AD. However, as a long-term medication is required for AD, which is a chronic disease with complex pathogenic mechanisms and a long disease course, the side effects of TZDs will substantially limit their application in AD treatment. Studies have demonstrated that rosiglitazone may lead to an increased risk of fractures (54), heart failure (55,56) and increased incidence of stroke (56); pioglitazone may lead to fractures and bladder cancer (54,57); and troglitazone may induce severe hepatotoxicity (58). Therefore, there is a need for TZD replacement with safer and effective drugs presenting mild side effects and PPAR $\gamma$ -agonistic effects in the study of AD therapies.

Ginseng is a natural herbal remedy that has been used in China over several millennia (1). Ginseng has multi-target therapeutic and pharmacological effects in central nervous system, which have been well-demonstrated in the clinical practice (59). Ginsenosides, which mainly include Rb1, Rb2, Rb3, Rc, Rd, Re, Rg1 and Rg2, are the main components of ginseng (60). In particular, ginsenoside Rg1 is one of the most studied and representative ginsenoside components in the field of AD treatment (61). Previous studies have observed that ginsenoside Rg1 may potentially activate PPAR $\gamma$  and facilitate A $\beta$  removal by enhancing the binding of PPAR $\gamma$  to target genes or by upregulating PPAR $\gamma$  expression (14,15). Accordingly, the present study further elucidated the mechanisms by which ginsenoside Rg1 affects PPAR $\gamma$ . The results of the present study suggested that ginsenoside Rg1 inhibits PPAR $\gamma$  phosphorylation by downregulating the expression of CDK5, thereby affecting the expression of PPAR $\gamma$  target genes.

Extracellular and intracellular A $\beta$  serve essential roles in the onset of AD (62). BACE1-mediated APP proteolysis produces a soluble  $\beta$ -fragment of the amyloid precursor protein and a C-terminal fragment containing 99 amino acids (C99). Subsequently, C99 is enzymatically cleaved by  $\gamma$ -secretase to generate APP intracellular domain and A $\beta$ ; the latter is released into the extracellular matrix (63,64) (Fig. 8). APP proteolysis also occurs in the endoplasmic reticulum and golgi apparatus (64,65), producing intracellular A $\beta$ . Gouras *et al* (66) reported that intraneuronal A $\beta$  immunoreactivity appeared to precede the deposition of both neurofibrillary tangles and senile plaques, indicating that intraneuronal accumulation of

A $\beta$  is an early event in the onset of AD. The neuron model of AD in this study was established with the addition of exogenous A $\beta$ , so exogenous and neuro-secreted A $\beta$  could not be distinguished, and this study only observed the effect of ginsenoside Rg1 on the intracellular A $\beta$  and did not investigate the changes in extracellular A $\beta$  levels.

This study demonstrated that Rg1 inhibited CDK5 expression. However, the mechanism remains unclear. The results of the present study suggested that ginsenoside Rg1 may affect CDK5 directly, or through other mechanisms; this needs to be investigated. The results of the present also demonstrated that exogenously added A $\beta$  increased CDK5 expression levels, aggravated PPAR $\gamma$  phosphorylation, decreased PPAR $\gamma$  expression levels, and affected the expression levels of the downstream PPAR $\gamma$  target genes *Ide* and *Bace1*. The exact mechanisms of these phenomena remain unclear and are subjects for future studies. Previous studies have observed a negative correlation between IDE expression and A $\beta$  levels in AD brains (67), and a decrease in IDE expression levels were also observed in an AD rat model established through the injection of A $\beta$ <sub>1-42</sub> in the hippocampus (15). These findings are consistent with those of the present study, which demonstrated decreased IDE expression levels in A $\beta$ -treated primary cultured hippocampal neurons. After treatment with ginsenoside Rg1, IDE expression levels increased and A $\beta$  levels decreased. Several possible reasons may account for these findings: i) The consumption of IDE through its effects on degradation of A $\beta$  exceeds the compensatory generation of IDE; ii) decreased IDE expression may consequently promote A $\beta$  generation; and iii) mutual interactions may exist between IDE and A $\beta$ , i.e., generated A $\beta$  affects IDE expression, whereas decreased IDE expression promotes an increase in A $\beta$  levels. Accordingly, further studies are required to verify these explanations. This study demonstrated that CDK5 mediates the ginsenoside Rg1 reduction of A $\beta$  levels by phosphorylating PPAR $\gamma$ . In addition to CDK5, other CDKs such as CDK7 and CDK9 also take part in PPAR $\gamma$  phosphorylation. A previous study has reported that CDK7 phosphorylates PPAR $\gamma$  at Ser112 to inhibit the activity of PPAR $\gamma$  (68). However, CDK9 increases PPAR $\gamma$  activity after phosphorylating PPAR $\gamma$  at Ser112 (69). Thus, further investigation is necessary into whether the phosphorylation of PPAR $\gamma$  by CDK7 and CDK9 is involved in the ginsenoside Rg1 reduction of A $\beta$  levels. Additionally, the results of the present study demonstrated that the protein and mRNA expression levels of PPAR $\gamma$  in the Rg1 group were higher compared with those in the control group. It was speculated this is due to the high concentrations of ginsenoside Rg1 used in the study, which were able to stimulate a significant response compared with the control.

There are several limitations to this study. In the study, no experiments such as chromatin immunoprecipitation RT-qPCR, were performed to confirm whether CDK5 directly regulates PPAR $\gamma$ . However, our previous study reported that CDK5 regulates PPAR $\gamma$  (21), and performed co-immunoprecipitation experiments to confirm that A $\beta$  promotes the binding of CDK5 to PPAR $\gamma$  (53). In addition, our previous study demonstrated that the PPAR $\gamma$  agonist pioglitazone inhibits PPAR $\gamma$  phosphorylation by inhibiting CDK5 expression, thereby promoting A $\beta$  degradation and reducing A $\beta$  production (53). Therefore, no PPAR $\gamma$  agonist

was used for comparison with ginsenoside Rg1 in this study. Since a CDK5 inhibitor was used in the study, no *in vivo* studies were conducted and only *in vitro* experiments were performed; therefore, the effects of ginsenoside Rg1 *in vivo* are unknown. Furthermore, since there are no available drugs that target CDK5, no positive-control drug was used in the study. A set of CDK5 overexpressing cells would allow for testing of the results of this study; unfortunately, CDK5 overexpression experiments were not performed due to limitations on time and funding.

In conclusion, the results of the present study suggested that ginsenoside Rg1 inhibits PPAR $\gamma$  phosphorylation possibly through the downregulation of CDK5 expression, thereby affecting the expression of PPAR $\gamma$  target genes (*Ide* and *Bace1*) and decreasing A $\beta$  levels through the promotion of A $\beta$  degradation and reduction of A $\beta$  synthesis, which ultimately provides neuroprotective effects against AD.

## Acknowledgements

Not applicable.

## Funding

This study was supported by the Chinese Postdoctoral Science Foundation (grant no. 2017M623191), the Natural Science Foundation of Shaanxi Province (grant no. 2017JQ8039) and the Foundation of The Second Affiliated Hospital of the Xi'an Jiaotong University [grant no. YJ(ZD)201517].

## Availability of data and materials

All data generated or analyzed during this study are included in this published article.

## Authors' contributions

QQ, XL and JF designed the study and wrote the manuscript. QQ, JH, ML and BZ performed the experiments. QQ and JH collected and analyzed the data. All authors read and approved the final manuscript.

## Ethics approval and consent to participate

All experimental procedures in the present study were approved by the Ethics Committee of The Second Affiliated Hospital of Xi'an Jiaotong University.

## Patient consent for publication

Not applicable.

## Competing interests

The authors declare that they have no competing interests.

## References

- Chen CF, Chiou WF and Zhang JT: Comparison of the pharmacological effects of Panax ginseng and Panax quinquefolium. *Acta Pharmacol Sin* 29: 1103-1108, 2008.
- Nie L, Xia J, Li H, Zhang Z, Yang Y, Huang X, He Z, Liu J and Yang X: Ginsenoside Rg1 ameliorates behavioral abnormalities and modulates the hippocampal proteomic change in triple transgenic mice of Alzheimer's disease. *Oxid Med Cell Longev* 2017: 6473506, 2017.
- Mu JS, Lin H, Ye JX, Lin M and Cui XP: Rg1 exhibits neuroprotective effects by inhibiting the endoplasmic reticulum stress-mediated c-Jun N-terminal protein kinase apoptotic pathway in a rat model of Alzheimer's disease. *Mol Med Rep* 12: 3862-3868, 2015.
- Liu QA, Kou JP and Yu BY: Ginsenoside Rg1 protects against hydrogen peroxide-induced cell death in PC12 cells via inhibiting NF- $\kappa$ B activation. *Neurochem Int* 58: 119-125, 2011.
- Huang T, Fang F, Chen L, Zhu Y, Zhang J, Chen X and Yan SS: Ginsenoside Rg1 attenuates oligomeric A $\beta$ (1-42)-induced mitochondrial dysfunction. *Curr Alzheimer Res* 9: 388-395, 2012.
- Tanzi RE, Moir RD and Wagner SL: Clearance of Alzheimer's A $\beta$  peptide: The many roads to perdition. *Neuron* 43: 605-608, 2004.
- Álvarez-Arellano L, Pedraza-Escalona M, Blanco-Ayala T, Camacho-Concha N, Cortés-Mendoza J, Pérez-Martínez L and Pedraza-Alva G: Autophagy impairment by caspase-1-dependent inflammation mediates memory loss in response to  $\beta$ -amyloid peptide accumulation. *J Neurosci Res* 96: 234-246, 2018.
- Seino Y, Kawarabayashi T, Wakasaya Y, Watanabe M, Takamura A, Yamamoto-Watanabe Y, Kurata T, Abe K, Ikeda M, Westaway D, *et al*: Amyloid  $\beta$  accelerates phosphorylation of tau and neurofibrillary tangle formation in an amyloid precursor protein and tau double-transgenic mouse model. *J Neurosci Res* 88: 3547-3554, 2010.
- Vargas LM, Leal N, Estrada LD, González A, Serrano F, Araya K, Gysling K, Inestrosa NC, Pasquale EB and Alvarez AR: EphA4 activation of c-Abl mediates synaptic loss and LTP blockade caused by amyloid- $\beta$  oligomers. *PLoS One* 9: e92309, 2014.
- Ibi D, Tsuchihashi A, Nomura T and Hiramatsu M: Involvement of GAT2/BGT-1 in the preventive effects of betaine on cognitive impairment and brain oxidative stress in amyloid  $\beta$  peptide-injected mice. *Eur J Pharmacol* 842: 57-63, 2019.
- Hooshmandi E, Ghasemi R, Iloun P and Moosavi M: The neuroprotective effect of agmatine against amyloid  $\beta$ -induced apoptosis in primary cultured hippocampal cells involving ERK, Akt/GSK-3 $\beta$ , and TNF- $\alpha$ . *Mol Biol Rep* 46: 489-496, 2019.
- Schirinzi T, Di Lorenzo F, Sancesario GM, Di Lazzaro G, Ponzo V, Pisani A, Mercuri NB, Koch G and Martorana A: Amyloid-mediated cholinergic dysfunction in motor impairment related to Alzheimer's disease. *J Alzheimers Dis* 64: 525-532, 2018.
- Ali T, Yoon GH, Shah SA, Lee HY and Kim MO: Osmotin attenuates amyloid beta-induced memory impairment, tau phosphorylation and neurodegeneration in the mouse hippocampus. *Sci Rep* 5: 11708, 2015.
- Chen LM, Lin ZY, Zhu YG, Lin N, Zhang J, Pan XD and Chen XC: Ginsenoside Rg1 attenuates  $\beta$ -amyloid generation via suppressing PPAR $\gamma$ -regulated BACE1 activity in N2a-APP695 cells. *Eur J Pharmacol* 675: 15-21, 2012.
- Quan Q, Wang J, Li X and Wang Y: Ginsenoside Rg1 decreases A $\beta$ 1-42 level by upregulating PPAR $\gamma$  and IDE expression in the hippocampus of a rat model of Alzheimer's disease. *PLoS One* 8: e59155, 2013.
- Liu C, Zhai X, Zhao B, Wang Y and Xu Z: Cyclin I-like (CCNI2) is a Cyclin-dependent kinase 5 (CDK5) activator and is involved in cell cycle regulation. *Sci Rep* 7: 40979, 2017.
- Su SC and Tsai LH: Cyclin-dependent kinases in brain development and disease. *Annu Rev Cell Dev Biol* 27: 465-491, 2011.
- Lopes JP and Agostinho P: Cdk5: Multitasking between physiological and pathological conditions. *Prog Neurobiol* 94: 49-63, 2011.
- Wilkaniec A, Czapski GA and Adamczyk A: Cdk5 at crossroads of protein oligomerization in neurodegenerative diseases: Facts and hypotheses. *J Neurochem* 136: 222-233, 2016.
- Choi JH, Banks AS, Estall JL, Kajimura S, Boström P, Laznik D, Ruas JL, Chalmers MJ, Kamenecka TM, Blüher M, *et al*: Anti-diabetic drugs inhibit obesity-linked phosphorylation of PPAR $\gamma$  by Cdk5. *Nature* 466: 451-456, 2010.
- Quan Q, Qian Y, Li X and Li M: CDK5 participates in amyloid- $\beta$  production by regulating PPAR $\gamma$  phosphorylation in primary rat hippocampal neurons. *J Alzheimers Dis* 71: 443-460, 2019.
- Vadukul DM, Gbajumo O, Marshall KE and Serpell LC: Amyloidogenicity and toxicity of the reverse and scrambled variants of amyloid- $\beta$  1-42. *FEBS Lett* 591: 822-830, 2017.

23. Yang EJ, Ahn S, Ryu J, Choi MS, Choi S, Chong YH, Hyun JW, Chang MJ and Kim HS: Phloroglucinol attenuates the cognitive deficits of the 5XFAD mouse model of Alzheimer's disease. *PLoS One* 10: e0135686, 2015.
24. Li Y, Guan Y, Wang Y, Yu CL, Zhai FG and Guan LX: Neuroprotective effect of the ginsenoside Rg1 on cerebral ischemic injury in vivo and in vitro is mediated by PPAR $\gamma$ -regulated antioxidative and anti-inflammatory pathways. *Evid Based Complement Alternat Med* 2017: 7842082, 2017.
25. Manser C, Vagnoni A, Guillot F, Davies J and Miller CC: Cdk5/p35 phosphorylates lemur tyrosine kinase-2 to regulate protein phosphatase-1C phosphorylation and activity. *J Neurochem* 121: 343-348, 2012.
26. Mandrekar-Colucci S, Karlo JC and Landreth GE: Mechanisms underlying the rapid peroxisome proliferator-activated receptor- $\gamma$ -mediated amyloid clearance and reversal of cognitive deficits in a murine model of Alzheimer's disease. *J Neurosci* 32: 10117-10128, 2012.
27. Houseknecht KL, Cole BM and Steele PJ: Peroxisome proliferator-activated receptor gamma (PPARgamma) and its ligands: A review. *Domest Anim Endocrinol* 22: 1-23, 2002.
28. Echeverría F, Valenzuela R, Catalina Hernandez-Rodas M and Valenzuela A: Docosahexaenoic acid (DHA), a fundamental fatty acid for the brain: New dietary sources. *Prostaglandins Leukot Essent Fatty Acids* 124: 1-10, 2017.
29. Echeverría F, Ortiz M, Valenzuela R and Videla LA: Long-chain polyunsaturated fatty acids regulation of PPARs, signaling: Relationship to tissue development and aging. *Prostaglandins Leukot Essent Fatty Acids* 114: 28-34, 2016.
30. Lin N, Chen LM, Pan XD, Zhu YG, Zhang J, Shi YQ and Chen XC: Tripchlorolide attenuates  $\beta$ -amyloid generation via suppressing PPAR $\gamma$ -regulated BACE1 activity in N2a/APP695 cells. *Mol Neurobiol* 53: 6397-6406, 2016.
31. Sadleir KR, Eimer WA, Cole SL and Vassar R: A $\beta$  reduction in BACE1 heterozygous null 5XFAD mice is associated with transgenic APP level. *Mol Neurodegener* 10: 1, 2015.
32. Du J, Zhang L, Liu SB, Zhang C, Huang XQ, Li J, Zhao NM and Wang Z: PPARgamma transcriptionally regulates the expression of insulin-degrading enzyme in primary neurons. *Biochem Biophys Res Commun* 383: 485-490, 2009.
33. Vingtdoux V, Chandakkar P, Zhao H, Blanc L, Ruiz S and Marambaud P: CALHM1 ion channel elicits amyloid- $\beta$  clearance by insulin-degrading enzyme in cell lines and in vivo in the mouse brain. *J Cell Sci* 128: 2330-2338, 2015.
34. Delerive P, Fruchart JC and Staels B: Peroxisome proliferator-activated receptors in inflammation control. *J Endocrinol* 169: 453-459, 2001.
35. Decourt B, Lahiri DK and Sabbagh MN: Targeting tumor necrosis factor alpha for Alzheimer's disease. *Curr Alzheimer Res* 14: 412-425, 2017.
36. Mendiola AS and Cardona AE: The IL-1 $\beta$  phenomena in neuro-inflammatory diseases. *J Neural Transm (Vienna)* 125: 781-795, 2018.
37. Haddick PC, Larson JL, Rathore N, Bhangale TR, Phung QT, Srinivasan K, Hansen DV, Lill JR; Alzheimer's Disease Genetic Consortium (ADGC); Alzheimer's Disease Neuroimaging Initiative (ADNI), *et al*: A common variant of IL-6R is associated with elevated IL-6 pathway activity in Alzheimer's disease brains. *J Alzheimers Dis* 56: 1037-1054, 2017.
38. Cifuentes D, Poitvein M, Bonnin P, Ngkelo A, Kubis N, Merkulova-Rainon T and Lévy BI: Inactivation of nitric oxide synthesis exacerbates the development of Alzheimer disease pathology in APPS1 mice (Amyloid Precursor Protein/Presenilin-1). *Hypertension* 70: 613-623, 2017.
39. Moussa C, Hebron M, Huang X, Ahn J, Rissman RA, Aisen PS and Turner RS: Resveratrol regulates Neuro-inflammation and induces adaptive immunity in Alzheimer's disease. *J Neuroinflammation* 14: 1, 2017.
40. Spitzer P, Weinbeer J, Herrmann M, Oberstein TJ, Condić M, Lewczuk P, Kornhuber J and Maler JM: Analysis of surface levels of IL-1 receptors and macrophage scavenger receptor I in peripheral immune cells of patients with Alzheimer's disease. *J Geriatr Psychiatry Neurol* 32: 211-220, 2019.
41. de la Monte SM and Wands JR: Molecular indices of oxidative stress and mitochondrial dysfunction occur early and often progress with severity of Alzheimer's disease. *J Alzheimers Dis* 9: 167-181, 2006.
42. Zhang ZX, Li YB and Zhao RP: Epigallocatechin gallate attenuates  $\beta$ -Amyloid generation and oxidative stress involvement of PPAR $\gamma$  in N2a/APP695 cells. *Neurochem Res* 42: 468-480, 2017.
43. Silva-Abreu M, Calpena AC, Andrés-Benito P, Aso E, Romero IA, Roig-Cardes D, Gromnicova R, Espina M, Ferrer I, García ML and Male D: PPAR $\gamma$  agonist-loaded PLGA-PEG nanocarriers as a potential treatment for Alzheimer's disease: In vitro and in vivo studies. *Int J Nanomedicine* 13: 5577-5590, 2018.
44. Searcy JL, Phelps JT, Pancani T, Kadish I, Popovic J, Anderson KL, Beckett TL, Murphy MP, Chen KC, Blalock EM, *et al*: Long-term pioglitazone treatment improves learning and attenuates pathological markers in a mouse model of Alzheimer's disease. *J Alzheimers Dis* 30: 943-961, 2012.
45. Hamano T, Shirafuji N, Makino C, Yen SH, Kanaan NM, Ueno A, Suzuki J, Ikawa M, Matsunaga A, Yamamura O, *et al*: Pioglitazone prevents tau oligomerization. *Biochem Biophys Res Commun* 478: 1035-1042, 2016.
46. Dehghani L, Meamar R, Askari G, Khorvash F, Shaygannejad V, Pour AF and Javanmard SH: The effect of pioglitazone on the Alzheimer's disease-induced apoptosis in human umbilical vein endothelial cells. *Int J Prev Med* 4 (Suppl 2): S205-S210, 2013.
47. Escribano L, Simón AM, Gimeno E, Cuadrado-Tejedor M, de Maturana RL, García-Osta A, Ricobaraza A, Pérez-Mediavilla A, Del Río J and Frechilla D: Rosiglitazone rescues memory impairment in Alzheimer's transgenic mice: Mechanisms involving a reduced amyloid and tau pathology. *Neuropsychopharmacology* 35: 1593-1604, 2010.
48. Chiang MC, Nicol CJ, Cheng YC, Lin KH, Yen CH and Lin CH: Rosiglitazone activation of PPAR $\gamma$ -dependent pathways is neuroprotective in human neural stem cells against amyloid-beta-induced mitochondrial dysfunction and oxidative stress. *Neurobiol Aging* 40: 181-190, 2016.
49. Toledo EM and Inestrosa NC: Activation of Wnt signaling by lithium and rosiglitazone reduced spatial memory impairment and neurodegeneration in brains of an APPswe/PSEN1 $\Delta$ E9 mouse model of Alzheimer's disease. *Mol Psychiatry* 15: 272-285, 2010.
50. Strum JC, Shehee R, Virley D, Richardson J, Mattie M, Selley P, Ghosh S, Nock C, Saunders A and Roses A: Rosiglitazone induces mitochondrial biogenesis in mouse brain. *J Alzheimers Dis* 11: 45-51, 2007.
51. Risner ME, Saunders AM, Altman JF, Ormandy GC, Craft S, Foley IM, Zvartau-Hind ME and Hosford DA; Rosiglitazone in Alzheimer's disease study group: Efficacy of rosiglitazone in a genetically defined population with mild-to-moderate Alzheimer's disease. *Pharmacogenomics J* 6: 246-254, 2006.
52. Combs CK, Johnson DE, Karlo JC, Cannady SB and Landreth GE: Inflammatory mechanisms in Alzheimer's disease: Inhibition of  $\beta$ -amyloid-stimulated proinflammatory responses and neurotoxicity by PPAR $\gamma$  agonists. *J Neurosci* 20: 558-567, 2000.
53. Quan Q, Qian Y, Li X and Li M: Pioglitazone reduces  $\beta$  amyloid levels via inhibition of PPAR $\gamma$  phosphorylation in a neuronal model of Alzheimer's disease. *Front Aging Neurosci* 11: 178, 2019.
54. Aubert RE, Herrera V, Chen W, Haffner SM and Pendergrass M: Rosiglitazone and pioglitazone increase fracture risk in women and men with type 2 diabetes. *Diabetes Obes Metab* 12: 716-721, 2010.
55. Home PD, Pocock SJ, Beck-Nielsen H, Gomis R, Hanefeld M, Jones NP, Komajda M and McMurray JJ; RECORD study group: Rosiglitazone evaluated for cardiovascular outcomes-an interim analysis. *New Engl J Med* 357: 28-38, 2007.
56. Wang AT and Smith SA: ACP Journal Club. In older patients, rosiglitazone was associated with increased risk for stroke, heart failure, and mortality compared with pioglitazone. *Ann Intern Med* 153: JC6-JC11, 2010.
57. Lewis JD, Ferrara A, Peng T, Hedderson M, Bilker WB, Quesenberry CP, Vaughn DJ, Nessel L, Selby J and Strom BL: Risk of bladder cancer among diabetic patients treated with pioglitazone interim report of a longitudinal cohort study. *Diabetes Care* 34: 916-922, 2011.
58. Toyota T and Ueno Y: Clinical effect and side effect of troglitazone. *Nihon Rinsho* 58: 376-382, 2000.
59. Kim HJ, Kim P and Shin CY: A comprehensive review of the therapeutic and pharmacological effects of ginseng and ginsenosides in central nervous system. *J Ginseng Res* 37: 8-29, 2013.
60. Zhang S, Sun H, Wang C, Zheng X, Jia X, Cai E and Zhao Y: Comparative analysis of active ingredients and effects of the combination of Panax ginseng and Ophiopogon japonicus at different proportions on chemotherapy-induced myelosuppression mouse. *Food Funct* 10: 1563-1570, 2019.

61. Kim MH, Kim SH and Yang WM: Mechanisms of action of phytochemicals from medicinal herbs in the treatment of Alzheimer's disease. *Planta Med* 80: 1249-1258, 2014.
62. LaFerla FM, Green KN and Oddo S: Intracellular amyloid-beta in Alzheimer's disease. *Nat Rev Neurosci* 8: 499-509, 2007.
63. Vassar R, Bennett BD, Babu-Khan S, Kahn S, Mendiaz EA, Denis P, Teplow DB, Ross S, Amarante P, Loeloff R, *et al*: Beta-secretase cleavage of Alzheimer's amyloid precursor protein by the transmembrane aspartic protease BACE. *Science* 286: 735-741, 1999.
64. Yu G, Nishimura M, Arawaka S, Levitan D, Zhang L, Tandon A, Song YQ, Rogaeva E, Chen F, Kawarai T, *et al*: Nicastrin modulates presenilin-mediated notch/glp-1 signal transduction and betaAPP processing. *Nature* 407: 48-54, 2000.
65. Xu H, Sweeney D, Wang R, Thinakaran G, Lo AC, Sisodia SS, Greengard P and Gandy S: Generation of Alzheimer  $\beta$ -amyloid protein in the trans-Golgi network in the apparent absence of vesicle formation. *Proc Natl Acad Sci USA* 94: 3748-3752, 1997.
66. Gouras GK, Tsai J, Naslund J, Vincent B, Edgar M, Checler F, Greenfield JP, Haroutunian V, Buxbaum JD, Xu H, *et al*: Intraneuronal A $\beta$ 42 accumulation in human brain. *Am J Pathol* 156: 15-20, 2000.
67. Pérez A, Morelli L, Cresto JC and Castano EM: Degradation of soluble amyloid  $\beta$ -peptides 1-40, 1-42, and the Dutch variant 1-40Q by insulin degrading enzyme from Alzheimer disease and control brains. *Neurochem Res* 25: 247-255, 2000.
68. Helenius K, Yang Y, Alasaari J and Mäkelä TP: Mat1 inhibits peroxisome proliferator-activated receptor  $\gamma$ -mediated adipocyte differentiation. *Mol Cell Biol* 29: 315-323, 2009.
69. Iankova I, Petersen RK, Annicotte JS, Chavey C, Hansen JB, Kratchmarova I, Sarruf D, Benkirane M, Kristiansen K and Fajas L: Peroxisome proliferator-activated receptor gamma recruits the positive transcription elongation factor b complex to activate transcription and promote adipogenesis. *Mol Endocrinol* 20: 1494-1505, 2006.



This work is licensed under a Creative Commons Attribution-NonCommercial-NoDerivatives 4.0 International (CC BY-NC-ND 4.0) License.